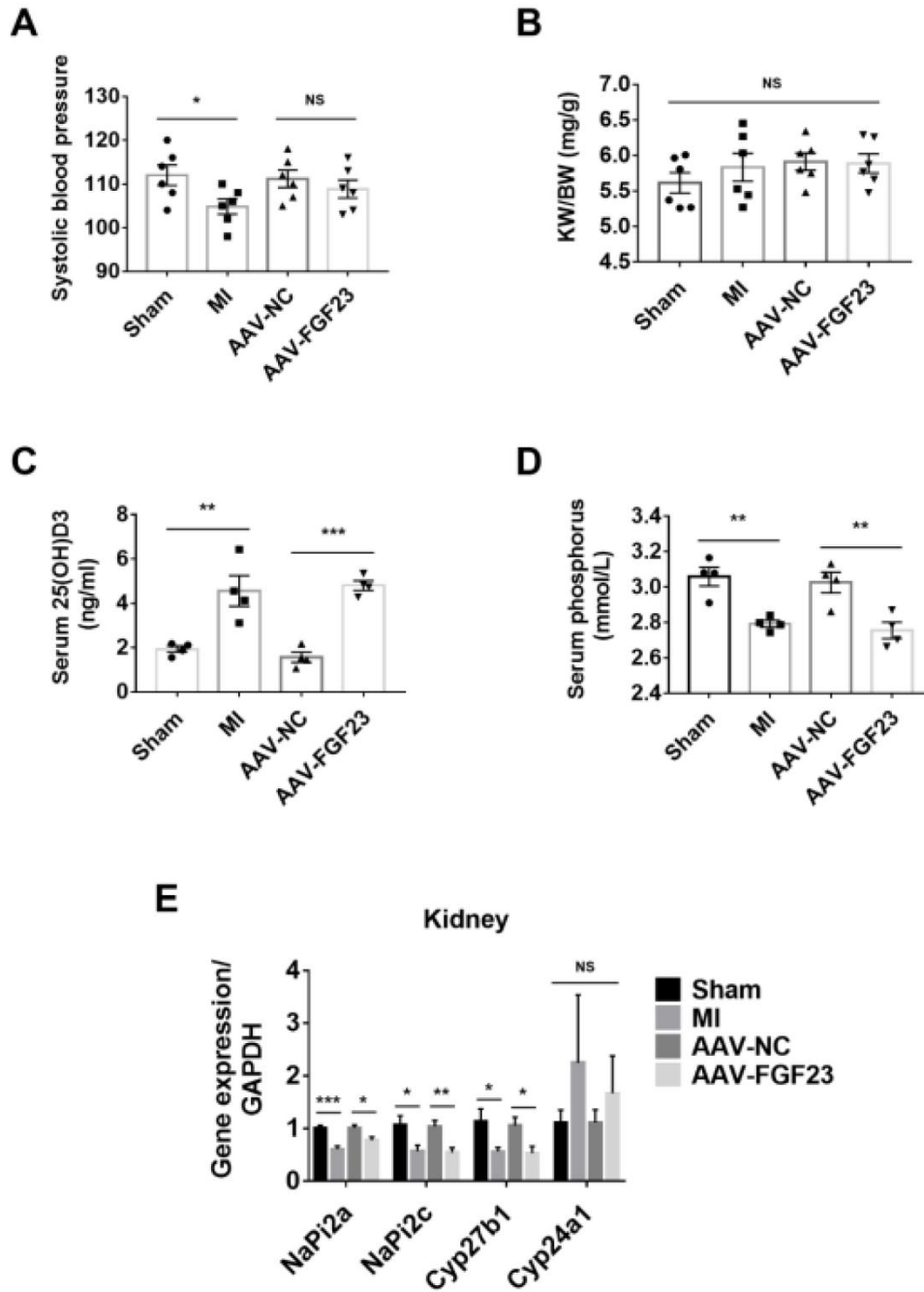
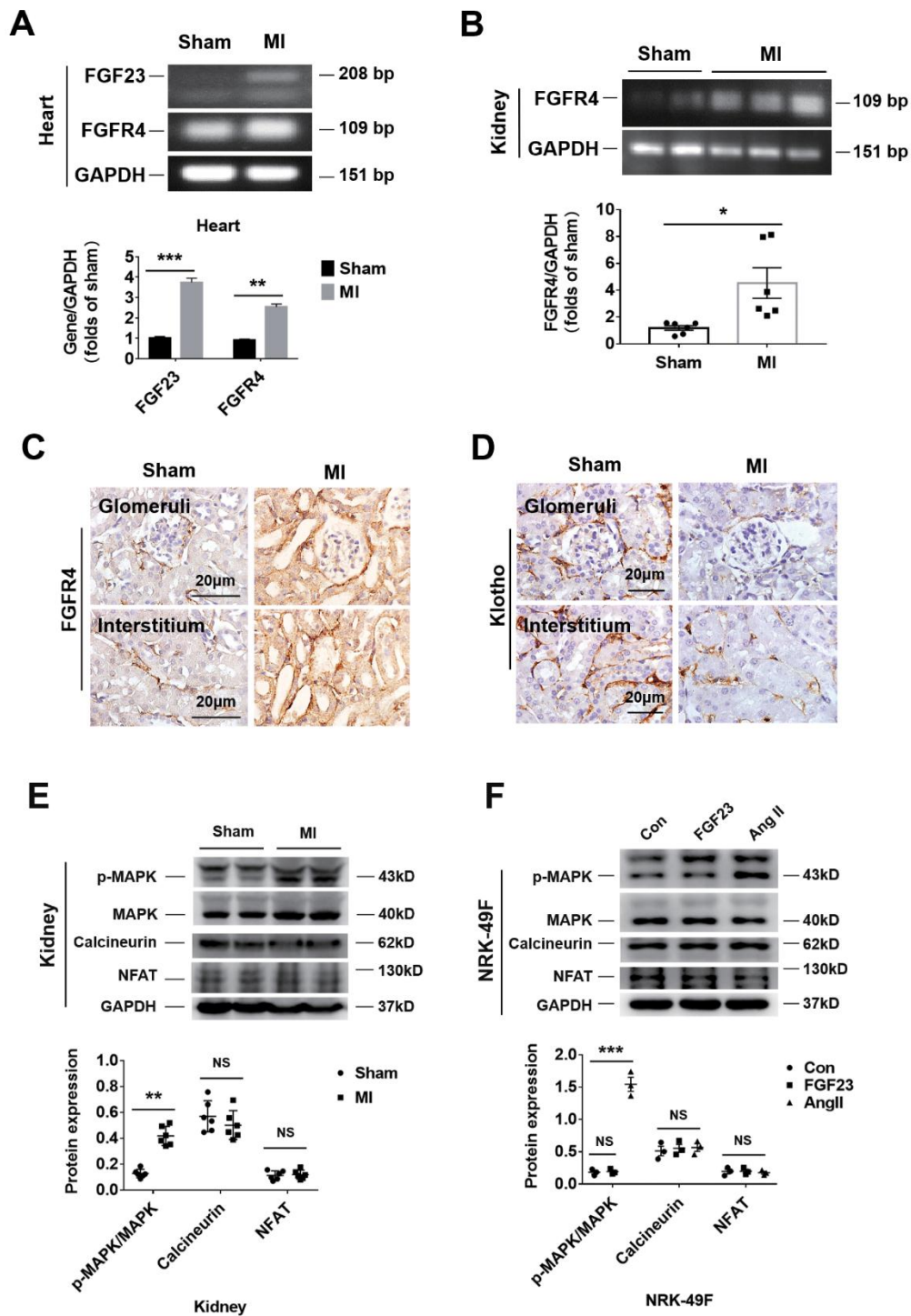


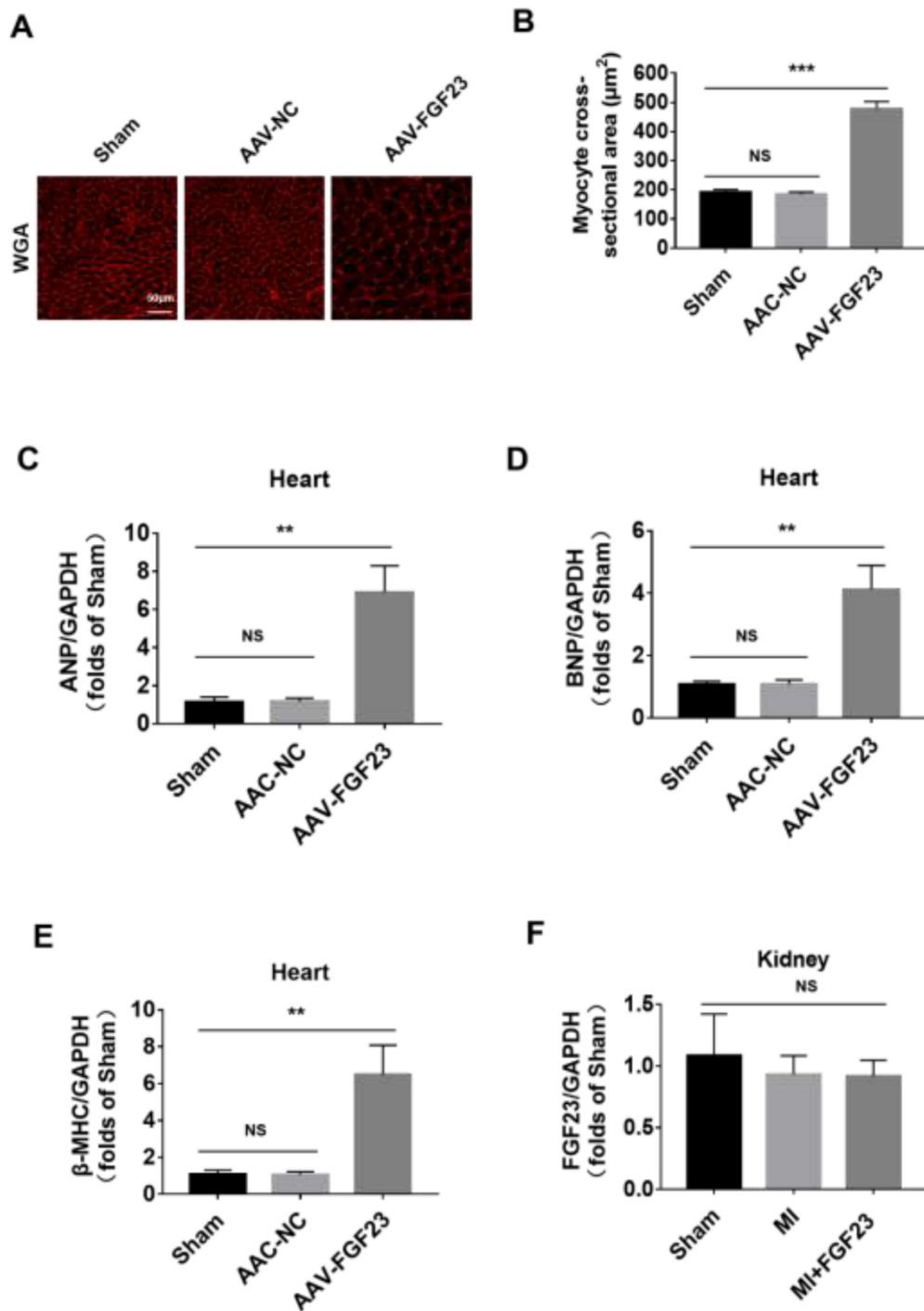
SUPPLEMENTARY FIGURES



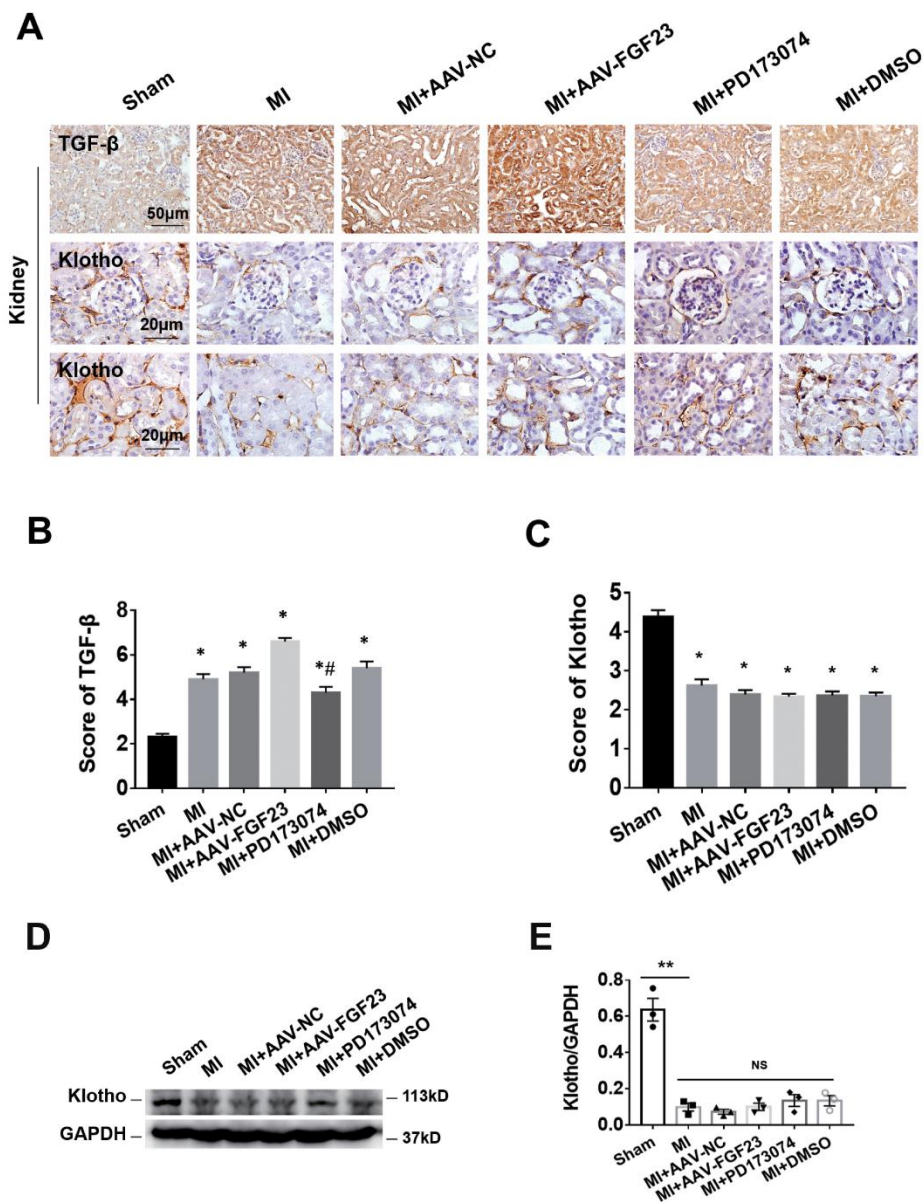
Supplementary Figure 1. The effects of MI or myocardial overexpression of FGF23 on hemodynamics, serological indicators and kidney related gene expression. (A) Systolic blood pressure. n = 6 per group. (B) Kidney weight/body weight ratio. n = 6 per group. Serum 25(OH)D3 (C) and serum phosphorus D (D) levels were measured by ELISA. n = 4 per group. (E) Quantitative real-time PCR for Napi2a, Napi2c, Cyp27b1 and Cyp24a1 mRNA in the kidneys. n = 6 per group, respectively. * $P < 0.05$; ** $P < 0.01$; *** $P < 0.001$; NS, no statistical significance; Data are means \pm SE.



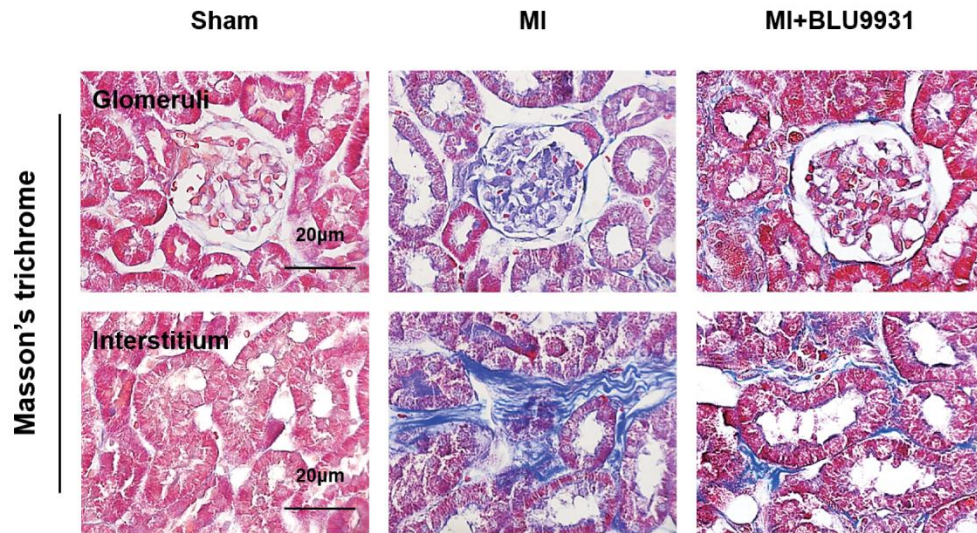
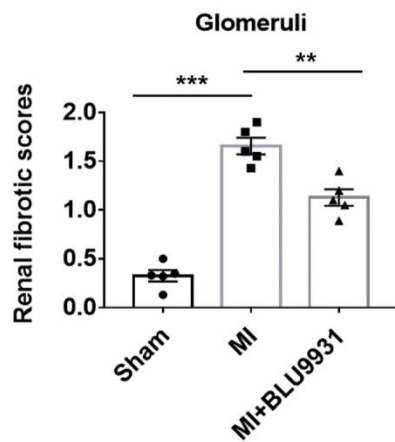
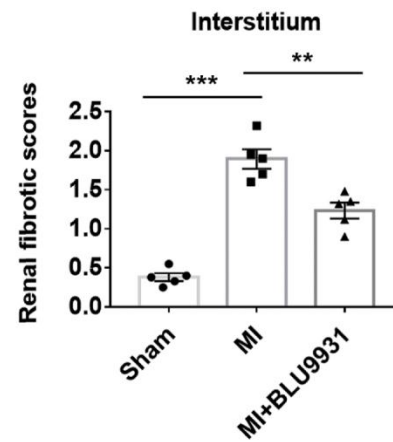
Supplementary Figure 2. FGF receptor 4 (FGFR4) was upregulated in the heart and kidneys and MAPK pathway was activated in the kidneys after induction of MI for 12 weeks. (A) Routine PCR and quantitative real-time PCR for FGF23 and FGFR4 mRNA in the heart. $n = 6$ per group. (B) Routine PCR and quantitative real-time PCR for FGFR4 mRNA in the kidneys. $n = 6$ per group, respectively. (C) Immunohistochemical staining displayed FGFR4 protein expression and localization in both the glomeruli and renal tubules. (D) Immunohistochemical staining showed reduced Klotho expression in the renal tubules of CRS mice compared with sham mice. (E) Western blot and semi-quantitative assessment of p-MAPK, MAPK, calcineurin and NFAT in the kidneys of CRS mice. $n = 6$ per group. (F) Western blot and semi-quantitative assessment of p-MAPK, MAPK, calcineurin and NFAT in cultured NRK-49F fibroblast cell line. $n = 3$ per group. * $P < 0.05$; ** $P < 0.01$; *** $P < 0.001$; NS, no statistical significance; Data are means \pm SE.



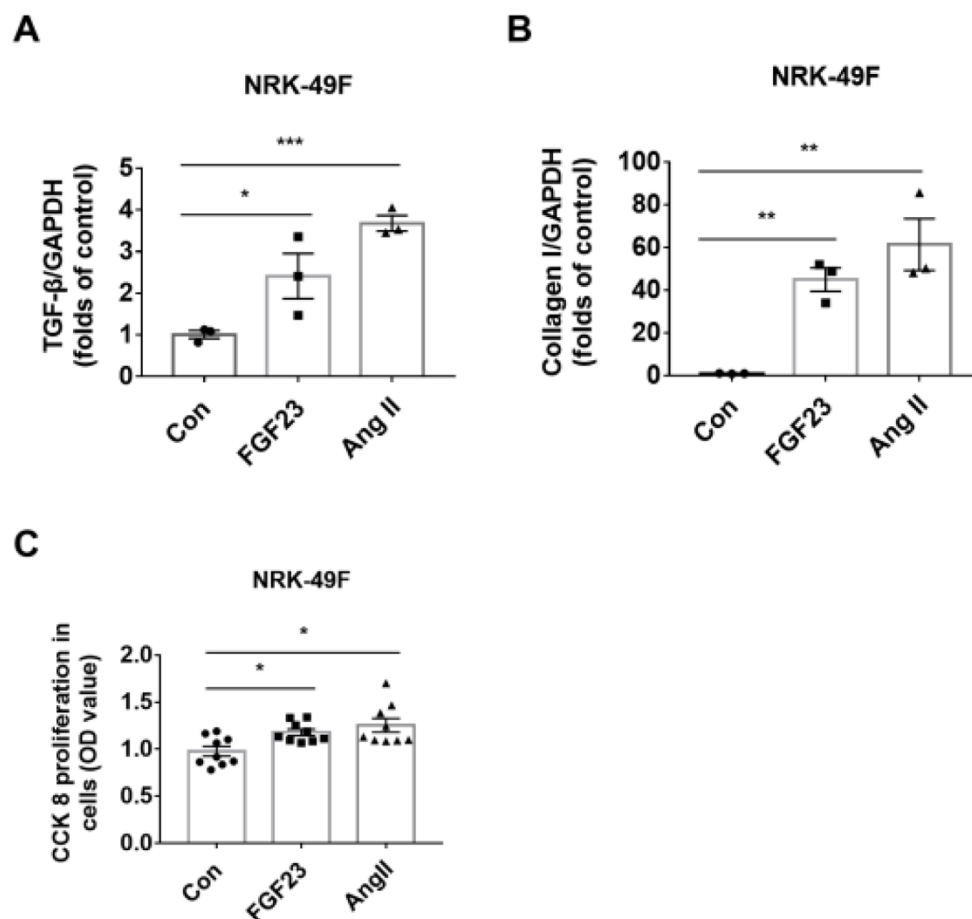
Supplementary Figure 3. Intramyocardial injection of FGF23 induced cardiac hypertrophy in mice. (A) The result of WGA-stained sections demonstrated that FGF23-induced cardiac hypertrophy. (B) Intramyocardial injection of FGF23 induced significantly increased cross-sectional surface area of individual cardiomyocytes. 20 cells from each animal were used to calculate its mean value of cross surface area of myocytes. Real-time PCR for ANP (C), BNP (D), β-MHC (E), and FGF23 (F). $n = 20$ in B, $n = 6$ in (C–F). $**P < 0.01$; $***P < 0.001$; NS, no statistical significance; Data are means \pm SE.



Supplementary Figure 4. Cardiac overexpression of FGF23 upregulated TGF- β and downregulated Klotho in the kidneys of mice with cardiorenal syndrome. Immunohistochemical staining was performed to detect renal expression of TGF- β and Klotho. (A) Representative images of TGF- β and Klotho immunostaining. (B) Semi-quantitative assessment of TGF- β . (C) Semi-quantitative assessment of Klotho. # $P < 0.05$ vs. the MI+AAV-FGF23 group, $n = 5$ per group. (D) Western blot of Klotho. (E) Semi-quantitative assessment of Klotho. $n = 3$ per group. * $P < 0.05$; ** $P < 0.01$; NS, no statistical significance; Data are means \pm SE.

A**B****C**

Supplementary Figure 5. FGFR4 antagonist BLU9931 also significantly inhibited MI-induced renal fibrosis. (A) Representative photomicrographs of renal fibrosis detected by Masson's trichrome stain in sham, MI and MI+BLU9931 groups. (B, C) Semi-quantitative assessment of glomerular and interstitial fibrosis. ** $P < 0.01$, *** $P < 0.001$. $n = 5$ per group. Data are means \pm SE.



Supplementary Figure 6. Real-time PCR of TGF-β and Collagen I in cultured NRK-49F fibroblast cell line (A, B). n = 3 per group. (C) The result of CCK-8 showed that FGF23 promoted fibroblast proliferation., n = 9 per group. Con, control; FGF23, fibroblast growth factor 23 (100 ng/mL); Ang II, angiotensin II (1 μM). **P* < 0.05; ***P* < 0.01; ****P* < 0.001; NS, no statistical significance; Data are means ± SE.